IOP Publishing Journal of Physics: Conference Series **59** (2007) 640–645
doi:10.1088/1742-6596/59/1/135 Eighth International Conference on Laser Ablation

Hydrodynamic multi-phase model for simulation of laser-induced non-equilibrium phase transformations

Alexey N. Volkov and Leonid V. Zhigilei*

Department of Materials Science and Engineering, University of Virginia
116 Engineer's Way, Charlottesville, VA 22904, USA

* E-mail: lz2n@virginia.edu

Abstract. A hydrodynamic model based on transport equations and semi-empirical multi-phase equations-of-state for metals is developed and applied to simulation of short pulse laser melting and resolidification. New computational algorithms are developed for modeling of two-phase zones of solid-liquid and liquid-gas coexistence, as well as for explicit tracking of interfaces between the phases. The model accounts for both heterogeneous and homogeneous melting mechanisms. A series of simulations are performed for bulk aluminum irradiated by a picosecond laser pulse at a wide range of laser fluence. The effect of non-equilibrium conditions and homogeneous melting on the melting/resolidification times and the maximum depth of melting is investigated. Three distinct stages are identified in the melting/resolidification process, namely, the fast homogeneous melting of the overheated surface region, a slower increase of the melting depth due to the advancement of the sharp melting front formed at the end of the homogeneous melting, and the reverse propagation of the liquid-crystal interface in recrystallization. Computational results are in a good qualitative agreement with the results of recent molecular dynamics simulations of laser melting.

1. Introduction

Recent advances in short pulse laser fabrication of micro- and nano-structures with resolution exceeding the optical diffraction limit [1,2,3] call for a better understanding of the processes responsible for surface modification. Most of the methods of sort pulse laser processing involve fast melting, active micro-scale flow of the molten material, and subsequent resolidification of the surface region. Although melting is a common and well studied phenomenon, the understanding of melting occurring under highly non-equilibrium conditions induced by fast laser energy deposition is far from being complete. Atomistic molecular dynamics (MD) simulations provide a unique opportunity to directly investigate the microscopic mechanisms and kinetics of the melting process under conditions of strong overheating [4] and transient thermoelastic deformations [5]. Due to the limited time- and length-scales accessible to the MD method, however, direct atomistic simulations of the complete sequence of melting – liquid flow – resolidification are not practical for real experimental conditions.

Continuum methods based on the integration of a system of partial differential equations are not suffering from the severe time- and length-scale limitations characteristic for atomistic models. The main challenge in application of continuum models to short-pulse laser processing is related to the necessity to develop phenomenological models and numerical implementations for the description of non-equilibrium processes. In particular, it has been demonstrated in MD simulations that short pulse laser melting involves both heterogeneous (propagation of the melting front) and homogeneous

(nucleation and growth of liquid regions inside the overheated crystal) mechanisms [5,6]. Therefore, an adequate continuum model for simulations of short pulse laser interactions with materials should account for both mechanisms of melting and the presence of two-phase regions of liquid-crystal coexistence. In most continuum models that have been applied to the simulation of laser melting so far, however, the coexistence of phases is not allowed and the description of the melting process is limited to the melting front propagation [7,8,9].

In this paper we present a new hydrodynamic multi-phase computational model which accounts for both heterogeneous and homogeneous phase transformations. The model is applied to the simulation of short pulse laser melting of a bulk aluminum target and the implications of the homogeneous melting mechanism for the kinetics of melting and the maximum melting depth are discussed.

2. Computational model

In this section we briefly describe a multi-phase computational model designed for simulations of short pulse laser interactions with metal targets. In the description given below we consider a bulk metal target with initial temperature T_0 and pressure p_0=0. X-axis is directed normal to the irradiated surface and the laser spot size is assumed to be much larger than the depth affected by the laser heating, allowing for a one-dimensional formulation of the problem. The laser energy absorption by the conduction band electrons and subsequent energy transfer to the lattice due to the electron-phonon coupling are described within the framework of the two-temperature model [10]. In order to take into account the homogeneous melting mechanism we assume that solid and liquid phases can coexist in an infinitesimal volume of material, with temperatures of both phases being equal (phases are in the local thermal equilibrium with each other). The difference in the velocities of the coexisting phases is assumed to be negligible. Then the motion, heat transfer and phase transformations can be described by the following set of one-dimensional multi-phase equations [11]:

$$\frac{\partial \alpha_1}{\partial t} + v\frac{\partial \alpha_1}{\partial x} = J_{\text{rel1}} + J_{v1},\ \alpha_2 = 1-\alpha_1,\ \frac{\partial}{\partial t}(\alpha_i\rho_i) + \frac{\partial}{\partial x}(\alpha_i\rho_i v) = J_{mi},\ i=1,2, \tag{1}$$

$$\frac{\partial}{\partial t}\left(\sum_{i=1}^{2}\alpha_i\rho_i v\right) + \frac{\partial}{\partial x}\left(\sum_{i=1}^{2}\alpha_i\left(\rho_i v^2 + p_i - \tau_{ai}\right)\right) = 0, \tag{2}$$

$$\frac{\partial}{\partial t}\left(\sum_{i=1}^{2}\alpha_i\rho_i\left(\varepsilon_{ai} + v^2/2\right)\right) + \frac{\partial}{\partial x}\left(\sum_{i=1}^{2}\alpha_i\left(v(\rho_i\left(\varepsilon_{ai} + v^2/2\right) + p_i - \tau_{ai}) + q_{ai}\right)\right) = Q_{ea}, \tag{3}$$

$$\frac{\partial}{\partial t}\left(\sum_{i=1}^{2}\alpha_i\rho_i\varepsilon_e\right) + \frac{\partial}{\partial x}\left(\sum_{i=1}^{2}\alpha_i\left(v\rho_i\varepsilon_e + q_{ai}\right)\right) = Q_{lp} - Q_{ea}. \tag{4}$$

Here subscripts 1 and 2 denote parameters and variables of solid and liquid phases, α_i and ρ_i are the volume fraction and the density of phase i, v is the velocity in x direction, $p_i=p_i(\rho_i,T_a)$ is the pressure of phase i. The internal specific energy of phase i is a function of the density of the corresponding phase and the temperature, T_a, common for both phases, $\varepsilon_{ai}=\varepsilon_{ai}(\rho_i,T_a)$. The internal specific energy of electrons is a function of the electron temperature T_e, $\varepsilon_e=\gamma T_e^2/2$. Variable $\tau_{ai}=(4/3)\mu_{ai}\partial v/\partial x$ is the viscous stress, $q_{ai}=-\kappa_{ai}\partial T_a/\partial x$ and $q_{ei}=-\kappa_{ei}(T_e/T_a)\partial T_e/\partial x$ are the heat fluxes in the lattice and electron subsystems. Term $Q_{lp}=I_L(t)\exp(-(x-x_0(t))/\lambda)/\lambda$ describes the absorption of laser irradiation by the electrons, where λ is the optical penetration depth, $x_0(t)$ is the coordinate of the surface at time t, and intensity $I_L(t)$ has a Gaussian temporal profile defined by the absorbed laser fluence F_L and pulse duration τ_L (full width at half maximum). Term $Q_{ea}=G(T_e-T_a)$ describes the electron-phonon coupling. Terms J_{rel1} and J_{v1} describe the changes in the volume fraction of the solid phase due to the relaxation of the pressure difference between the phases in the coexistence region and due to phase transformation, respectively. Term J_{mi} is the mass source for phase i associated with the phase transformation ($J_{m1}=-J_{m2}=\rho_1 J_{v1}$). In order to obtain J_{rel1}, we assume that the pressure relaxation in a two-phase region is fast and the pressure values in the coexisting phases are equal at all times. Then

the condition $p_1(\rho_1,T_a)= p_2(\rho_2,T_a)$ can be used for implicit calculation of J_{rel1}.

Equations of state (EOS) $p_i=p_i(\rho_i,T_a)$, $\varepsilon_{ai}=\varepsilon_{ai}(\rho_i,T_a)$ and the equilibrium melting temperature $T_m(p)$ are defined by a semi-empirical equation of state described in Ref. [12]. We neglect the electron contribution to the Helmholtz free energy in this EOS since non-equilibrium electron contribution is already accounted for by Eq. (4).

The term describing the phase transformation can be represented in the form $J_{v1}=V_m(T_f,p_f)\delta(x-x_f(t))+J_h(T_f,p_f)$, where the first and the second terms account for the heterogeneous and homogeneous melting, respectively, $x_f(t)$ is the current coordinate of the melting/solidification front, V_m is the velocity of the front with respect to the solid phase, $\delta(x)$ is the Dirac delta function, T_f and p_f are the temperature and pressure at the front. Heterogeneous melting takes place when the overheating $\Theta= T_f/T_m(p_f)-1$ is less than some critical value Θ_h. In this case the temperature dependence of the melting front velocity, V_m, can be described by the phenomenological theory [13] and, for small deviations from the equilibrium melting temperature, can be approximated by a linear relationship $V_m(T_f,p_f)=-\mu_m T_m(p_f)\Theta$ where μ_m is the kinetic coefficient.

If overheating Θ is higher than Θ_h, the homogeneous melting starts and liquid regions can nucleate and grow in the bulk of the crystal phase. For modeling of the homogeneous melting process we propose a simple model which is in agreement with the results of MD simulations of laser melting [5]:

$$J_h = -\begin{cases} 1/\tau_h & \Theta \ge \Theta_h \\ 1/\tau_h & |\Theta| < \Theta_h \quad \text{and} \quad 0<\alpha_2<1 \\ 0 & |\Theta| < \Theta_h \quad \text{and} \ \alpha_2 = 0 \ \text{or} \ \alpha_2 = 1 \end{cases}; \quad \tau_h = \begin{cases} \tau_{h0} \exp\left[-\chi_h(\Theta-\Theta_h)\right] & \Theta \ge \Theta_h \\ \tau_{h0}\Theta_h/\Theta & |\Theta| < \Theta_h \end{cases}, \quad (5)$$

where τ_h is the characteristic time of homogeneous melting. The case of $\Theta>\Theta_h$ corresponds to the fast homogeneous nucleation and growth of liquid regions, the case of $|\Theta|<\Theta_h$ corresponds to the slower melting or resolidification of already existing liquid regions with the rate proportional to Θ as in the case of heterogeneous melting. Parameter τ_{h0} can be estimated from the rate of homogeneous melting at the critical overheating Θ_h. Parameter χ_h must be sufficiently large in order to account for the fast increase of the rate of homogeneous melting with increase of Θ, as observed in MD simulations [5,6].

Equations (1)-(4) are suitable for modeling of phase transformations if the width of the two-phase region is sufficiently large. If this region is thin, it can be replaced by a sharp front separating pure liquid ($\alpha_2=1$) and solid ($\alpha_1=1$) regions. The conditions at the front can be found from equations (1)-(4) in the same way as the Rankine-Hugoniot conditions for the shock wave:

$$\rho_i(v_i - D_f) = J_m, \quad J_m v_1 + p_1 = J_m v_2 + p_2, \quad J_m\left(h_{a1} - \frac{\tau_{a1}}{\rho_1}\right) + q_{a1} = J_m\left(h_{a2} - \frac{\tau_{a2}}{\rho_2}\right) + q_{a2}, \quad q_{e1} = q_{e2}, \quad (6)$$

where D_f is the front velocity, $J_m=\rho_1 V_m(T_f,p_f)$ is the mass flux across the front, $h_{ai}=\varepsilon_{ai}+p_i/\rho_i$. Density, velocity and pressure are assumed to be discontinuous at the front. Assuming that free surface is non-evaporating and adiabatic, we have there: $p_i=0$, $q_{ai}=0$, $q_{ei}=0$, and $v_i=D_0$, where D_0 is the velocity of the free surface.

Equations (1)-(4) are solved numerically, using the modified MacCormack scheme [14] supplemented by an iterative procedure for calculation of J_{rel1}. In order to track the free surface and the melting/resolidification front, a new characteristic-based front tracking method is developed.

3. Results and discussion

The first test simulations with the multi-phase model described above are performed for aluminum target irradiated by short, from 1 to 300 ps, laser pulses at absorbed laser fluences ranging from 30 to 150 mJ/cm^2. The initial system has a temperature T_0 of 300 K and a density ρ_0 of 2711 kg/m^3 [12]. Other parameters of the system are as follows: $\rho_0\gamma$=92 J/(m^3·K), κ_{e1}=238 J/(K·m·s), G=4.9·10^{17} J/(kg·s·K) [15], κ_{e2}=91 J/(K·m·s) [16], $\kappa_{a1}=\kappa_{a2}$=1 J/(K·m·s), μ_{a1}=0, μ_{a2}=0.001 Pa·s [17], λ=15 nm, and Θ_h=0.2 [4]. Calculations based on a phenomenological model for the mobility of liquid-solid

interface [13] and EOS [12] yield μ_m=0.67 m/(s·K). Constants in Eq. (5) are taken to be τ_{h0}=9 ps and χ_h=4.

Spatial distributions of some of the hydrodynamic variables obtained in a simulation performed for F_L=90 mJ/cm^2 and τ_L=1 ps are shown in Fig. 1. Profiles of the volume fraction of the liquid phase, Fig. 1a, indicate that the size of the region of homogeneous melting increases rapidly during the first 4.5 ps of the simulation. At later time the liquid-crystal coexistence region becomes smaller and completely disappears by about 50 ps. The distributions of the mixture density $\rho=\alpha_1\rho_1+\alpha_2\rho_2$ (Fig. 1b) is smooth inside the two-phase region and on its boundaries. The difference in densities of solid and liquid phases in this region corresponds to the state when these phases are at the same pressure and temperature. The distribution of density becomes discontinuous at the melting front that appears only after the coexistence region collapses into a sharp interface and the melting/resolidification process continues by the heterogeneous mechanism (e.g. see a density plot for t=720 ps). During the initial stage of the melting process ($t\leq$36 ps) the minimum density is realized at some depth inside the liquid layer that approximately corresponds to the maximum negative pressure, Fig. 1c. A large local expansion of the melted region, up to 35% with respect to the initial specific volume, takes place during the initial stage of the relaxation of the laser-induced pressure (e.g. see a density plot for t=18 ps). After the transient pressure relaxation is completed, the density follows the EOS for zero pressure with the lowest density observed at the surface of the target, e.g. see plots for t=720 ps in Figs. 1b-d.

Distributions of the lattice temperature T_a are not monotonic but the maximum temperature is always realized at the free surface of the target, Fig. 1d. Local minima in the temperature plots correspond to the beginning of the coexistence region where the rate of the energy transfer to the latent heat of melting is the maximum (compare corresponding curves in Fig. 1a, 1b and 1d).

An increase in the laser fluence at a fixed pulse duration results in an increase in the amplitude of the negative (tensile) component of the pressure wave and a larger transient expansion the melted region. The increase in the negative pressure combined with the higher temperature of the surface region can lead to the conditions when the tensile stresses exceed the theoretical strength of the material at a given temperature, which can be found from the EOS [18]. These conditions correspond to the onset of the front spallation, when the surface region of the target disintegrates into two or

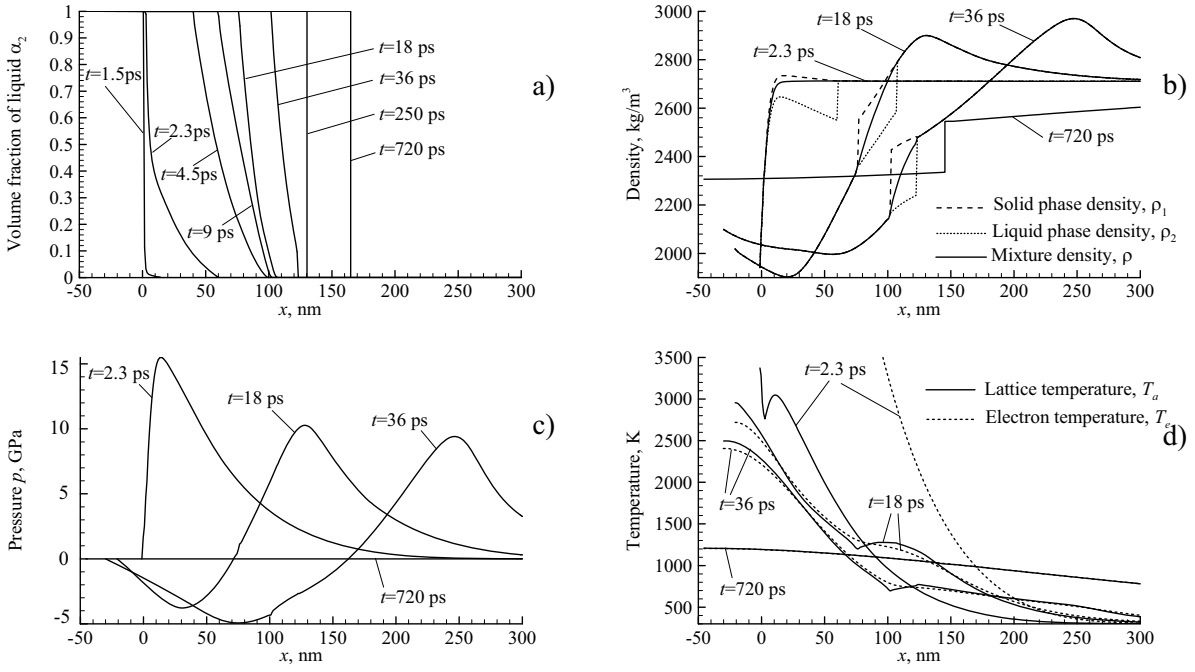

Figure 1. Distributions of liquid volume fraction (a), density (b), pressure (c) and temperature (d) in the bulk aluminum irradiated with a 1 ps laser pulse at an absorbed fluence of 90 mJ/cm^2.

several layers [19]. Experimental observations reported in Ref. [18] suggest that at the high deformation rates induced by picosecond laser pulses, the spallation takes place at tensile stresses approaching the theoretical strength of the material (for longer pulses the deformation rates associated with the propagation of the pressure wave are lower and the spallation stress may be much smaller than the theoretical strength due to a sufficient time for the sub-critical void nucleation and growth). The conditions for the front spallation are not achieved in the simulation performed at a fluence of 90 mJ/cm^2 and discussed above. We find, however, that in a simulation performed at a fluence of 150 mJ/cm^2 and the same pulse duration of 1 ps the spallation already takes place. In agreement with the results of earlier MD simulations [19], the conditions for the laser front spallation are always satisfied inside the melted region of the target.

The maximum width L_h of the two-phase region (where the homogeneous melting takes place) decreases with increasing pulse duration at a constant fluence, Fig. 2. This decrease can be explained by a slower lattice heating and, as a result, smaller region where the critical overheating, Θ_h, is exceeded. The value of L_h decreases rapidly as τ_L increases from 1 to 10 ps. With longer pulses and fluences exceeding 60 mJ/cm^2, the overheating of the surface region is largely controlled by the rates of the electronic heat conduction and the electron/phonon coupling, and the maximum width of the coexistence region is slowly decreasing with increasing pulse duration. For F_L=30 mJ/cm^2 the value of L_h drops rapidly at τ_L>100 ps and becomes zero at $\tau_L\approx$200 ps. The irradiation conditions of F_L=30 mJ/cm^2 and τ_L=200 ps are below the threshold for surface melting of the aluminum target. Similar drops at longer pulse durations are observed for $L_h(\tau_L)$ dependences shown in Fig. 2 for fluences of 60 and 90 mJ/cm^2. These results suggest that the two-phase region has a considerable size in a wide range of pulse durations and fluences and it can not be neglected except for the conditions very close to the threshold for melting.

Time evolution of the mass averaged melting depth, $L_m=\int\alpha_2\rho_2/\rho_0 dx$, is show for three different fluences in Fig. 3. Three distinct stages can be clearly identified in the melting/resolidification process. The process always starts from the fast homogeneous melting that lasts about 30-50 ps and accounts for a major fraction of the total melting at all fluences considered in this work. At low laser fluences, e.g. 30 mJ/cm^2 in Fig. 3, the fast homogeneous melting is immediately followed by resolidification. At higher fluences we observe an additional slower increase of the melting depth due to the advancement of the sharp liquid-crystal interface formed at the end of the homogeneous melting. At high laser fluences the duration of this heterogeneous stage of melting can be as long as nanoseconds. The long duration of heterogeneous melting can be explained by relatively weak temperature gradients observed late in the melting process, with temperature exceeding the equilibrium melting temperature T_m in a large surface region of the target (e.g. compare T_m=933 K at p=0 with the temperature distribution at 720 ps in Fig. 1d). The heterogeneous melting is followed by recrystallization that is always the longest stage of the melting-resolidification cycle. This picture of two-stage melting followed by recrystallization is in a good qualitative agreement with recent results of MD simulations obtained for Ni targets [6,19].

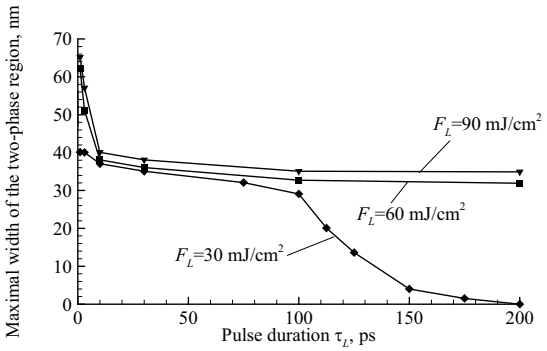

Figure 2. Maximum width L_h of the liquid-crystal coexistence region for laser pulses of

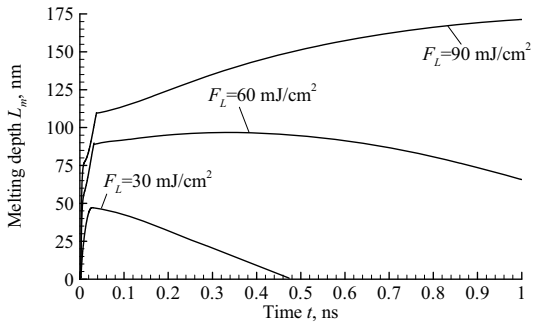

Figure 3. Melting depth L_m versus time obtained in simulations performed at laser fluences of 30,

various fluences F_L and pulse durations τ_L. 60, and 90 mJ/cm^2 and a pulse duration of 1 ps.

4. Summary

Hydrodynamic multi-phase model accounting for both heterogeneous and homogeneous melting mechanisms in short-pulse laser processing of metals is developed. The model includes new computational algorithms for the description of solid-liquid coexistence regions and an explicit tracking of interfaces between the phases. First application of the model for simulation of short pulse laser interactions with a bulk aluminum target demonstrate the profound effect the homogeneous melting mechanism has on the maximum melting depth and the time-scale of the melting process. The results obtained with the developed continuum model are found to be in a good qualitative agreement with the results of recent molecular dynamics simulations of laser melting of Ni targets. Quantitative comparison of the predictions of the continuum and MD models for the same material system and application of the continuum model to multidimensional phenomena are subjects of our current work.

Acknowledgments

The authors would like to thank Konstantin Khishchenko of the Institute for High Energy Densities, Russian Academy of Sciences, for helpful communication on the parameters for the equations of state. Financial support of this work is provided by the National Science Foundation through grant CTS-0348503 and by the Office of Naval Research through a sub-contract to the Electro-Optics Center, Penn State University.

References

[1] Chimmalgi A, Choi T Y, Grigoropoulos C P and Komvopoulos K 2003 *Appl. Phys. Lett*. **82** 1146

[2] Huang S M, Hong M H, Lukiyanchuk B and Chong T C 2003 *Appl. Phys.* A **77** 293

[3] Korte E, Koch J and Chichkov B N 2004 *Appl. Phys.* A **79** 879

[4] Luo S-N, Ahrens T J, Çağin T, Strachan A, Goddard III W A and Swift D C 2003 *Phys. Rev.* B **68** 134206

[5] Ivanov D S and Zhigilei L V 2003 *Phys. Rev.* B **68** 064114; ibid. *Phys. Rev. Lett.* **91** 105701

[6] Zhigilei L V, Ivanov D S, Leveugle E, Sadigh B and Bringa E M 2004 *Proc. SPIE* **5448** 505

[7] Yabe T, Xiao F and Utsumi T 2001 *J. Comput. Phys.* **169** 556

[8] Hoashi E, Yokomine T and Shimizu A 2002 *Num. Heat Transfer* A **41** 783

[9] Chowdhury I H and Xu X 2003 *Num. Heat Transfer* A **44** 219

[10] Anisimov S I, Kapeliovich B L and Perel'man T L 1974 *Sov. Phys. JETP*. **39** 375

[11] Drew D A and Passman S I 1998 *Theory of Multicomponent Fluids* (New York: Springer)

[12] Bushman A V, Kanel' G I , Ni A L and Fortov V E 1993 *Intense Dynamic Loading of Condensed Matter* (Washington: Tailor & Fransis) While implementing the equation of state described in this reference we identified several typographical errors which were corrected through private communication with Dr. Konstantin Khishchenko. The accuracy of our code was checked by reproducing the phase diagrams and experimental parameters given in the reference.

[13] Broughton J Q, Gilmer G H and Jackson K A 1982 *Phys. Rev. Lett*. **49** 1496

[14] MacCormack R W 1969 *AIAA Paper 69-354*

[15] Tas G and Maris H J 1994 *Rhys. Rev.* B **49** 15046

[16] Mills K C, Monaghan B J and Keene B J 1996 *Int. Mater. Rev*. **41** 209

[17] Wang L, Xiangfa L and Zhang Y 2004 *Physica* B **351** 208

[18] Eliezer S, Moshe E and Eliezer D 2002 *Laser and Particle Beams* **20** 87

[19] Leveugle E, Ivanov D S and Zhigilei L V 2004 *Appl. Phys.* A **79** 1643